Available online at www.sciencedirect.com
SCIENCE DIRECT®
Chemical Physics Letters 405 (2005) 265–269
CHEMICAL PHYSICS LETTERS
www.elsevier.com/locate/cplett

A practical approach to determine the handedness of chiral carbon nanotubes by electron diffraction

Zejian Liu [a], Lu-Chang Qin [a,b,*]

[a] Department of Physics and Astronomy, University of North Carolina at Chapel Hill, Campus Box 3255, Chapel Hill, NC 27599-3255, USA
[b] Curriculum in Applied and Materials Sciences, University of North Carolina at Chapel Hill, Chapel Hill, NC 27599-3255, USA

Received 8 December 2004; in final form 8 February 2005
Available online 9 March 2005

Abstract

A practical procedure has been proposed to determine the handedness of a carbon nanotube from its electron diffraction patterns. When a nanotube is twisted, the diffraction layer line spacings change, although the intensity distribution on the layer lines stays unchanged. The handedness can be assigned by observing the directions in which the principal layer lines shift under known direction of twisting and the twisting angle can be derived directly from the ratio of the diffraction layer line spacings. Simulated electron diffraction patterns of a carbon nanotube twisted both clockwise and counterclockwise are also presented as an example to corroborate the theoretical analysis.

---

1. Introduction

Carbon nanotubes are one of the most promising building blocks of nanoelectronics due to their novel electronic properties [1–3]. Depending on the chiral indices that define the perimeter of a carbon nanotube, the nanotube can be either metallic or semiconducting [4–6]. More interestingly, by twisting a normal carbon nanotube along the tubule axis, the electrical properties of the nanotube change noticeably [7].

For a complete determination of the atomic structure of a carbon nanotube, we need to specify the diameter, helicity, and handedness of the nanotube. Electron diffraction technique is a powerful technique in characterizing the atomic structure of both single-walled and multiwalled carbon nanotubes [8–14]. Using electron diffraction, we have been able to determine the diameter and helicity accurately and most of the studies have been dealing with deformation-free cylindrical nanotubes. Though there has been a rather large literature on the determination of diameter and helicity of carbon nanotubes, little has been available on the determination of the handedness of carbon nanotubes. A chiral carbon nanotube (u,v) can be right-handed or left-handed depending on the chiral indices. A carbon nanotube is defined as right-handed if the chiral indices u and v satisfy the condition of $u > v \geqslant 0$, whereas it is left-handed under the condition of $v > u \geqslant 0$.

In this Letter, we explore the possibility of characterizing the atomic structure of twisted carbon nanotubes by electron diffraction. After developing the kinematical theory of electron diffraction from twisted carbon nanotubes, we present a method to assign the handedness of carbon nanotubes by observing the shifting direction of the layer lines. In addition, the twisting angle can also be measured from the ratio of the diffraction layer line spacings. A series of simulated electron diffraction patterns from a carbon nanotube $(22,2)$ at different twisting angles are also given to corroborate our theoretical analysis.

---

[*] Corresponding author. Fax: +1 919 968 0480.
E-mail address: lcqin@physics.unc.edu (L.-C. Qin).

0009-2614/$ - see front matter © 2005 Elsevier B.V. All rights reserved.
doi:10.1016/j.cplett.2005.02.042

2. Theoretical considerations

Regardless if a carbon nanotube is twisted, the kinematical theory of electron diffraction can be applied to interpret the electron diffraction patterns due to the small atomic number of carbon atoms and the thin carbon layers in the nanotube [15,16]. The scattering amplitude for a normal carbon nanotube (without twisting) can be calculated by summing up all the contributions of its constituting helices

$$F(R,\Phi,l) = \sum_{j} \sum_{n,m=-\infty}^{+\infty} f J_n(\pi d R) \times \exp\left[\mathrm{i}n\left(\Phi+\frac{\pi}{2}\right)\right] \exp\left[-\mathrm{i}n\varphi_j + \frac{2\pi \mathrm{i} l z_j}{c}\right], \tag{1}$$

where f is the atomic scattering amplitude of carbon for electrons, d is the diameter of the carbon nanotube, c is the axial periodicity of the nanotube, (R,Φ,l) are the cylindrical coordinates in the reciprocal space, $(d/2,\varphi_j,z_j)$ are the relative cylindrical coordinates of the jth carbon helices revolving atom on the nanotube surface in the real space, $J_n(\pi dR)$ stands for the Bessel function of order n, and n, l and m are correlated by the selection rule [15]

$$\frac{l}{c} = \frac{n}{C} + \frac{m}{\Delta}, \tag{2}$$

with C and Δ being the pitch length and the axial distance of neighboring carbon atom pairs on one helix along the tubule axis, respectively.

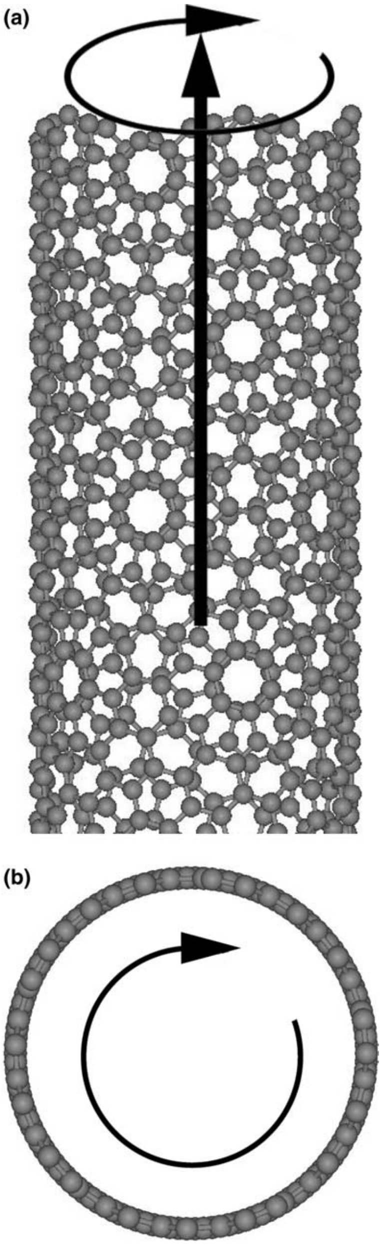

Fig. 1. (a) Schematic showing twisting a carbon nanotube about its tubule axis in side-view. (b) Viewed end-on. The circles with arrows around the tubule axis in (a) and (b) indicate a clockwise twisting seeing top-down.

Fig. 1a shows schematically the process of twisting a carbon nanotube: with one end fixed, the other end is twisted either clockwise or counter-clockwise about the tubule axis. Although energetically it is equivalent to twist an achiral (armchair or zigzag) nanotube in either direction, twisting a helical carbon nanotube in the direction of the helical lines is energetically easier than twisting it in the direction against the helical lines. Assuming that the cross-section of a twisted carbon nanotube remains circular as shown in Fig. 1b, i.e., the twisting angle is smaller than the threshold angle beyond which buckling of the nanotube begins to take place, the geometry of the twisted carbon nanotube in radial projection is illustrated in Fig. 2, where the carbon hexagons have been uniformly deformed. By twisting the carbon nanotube of chiral indices (u,v) an angle of $(u + 2v)\Delta\vartheta/(uM)$ about the tubule axis where M is the maximum common divisor of $(2u + v)$ and $(u + 2v)$, the pitch length of the twisted helices becomes $C^* = C/(1 + \Delta\vartheta/2\pi)$, although the axial distance between neighboring atoms along a helix stays the same, i.e., $\Delta^* = a_0 \sin(60^\circ - \alpha)$, where α is the helical angle of the untwisted nanotube and $a_0 = 0.246$ nm is the magnitude of the basis vector in the untwisted graphene. To make the twisted carbon nanotube still a periodic structure along the tubule axis, C^* and Δ^* have to satisfy the following condition:

$$\frac{C^*}{\Delta^*} = \frac{2(u^2+v^2+uv)}{(u+2v)\left(1+\dfrac{\Delta\vartheta}{2\pi}\right)} = \frac{p}{q}, \tag{3}$$

where p and q are integers, and we have expressed the helicity α by the chiral indices (u,v) for this nanotube. Eq. (3) requires that $\Delta\vartheta/2\pi = K_1/K_2$, where K_1 and K_2 are all integers. The selection rule for the twisted carbon nanotube can then be expressed as

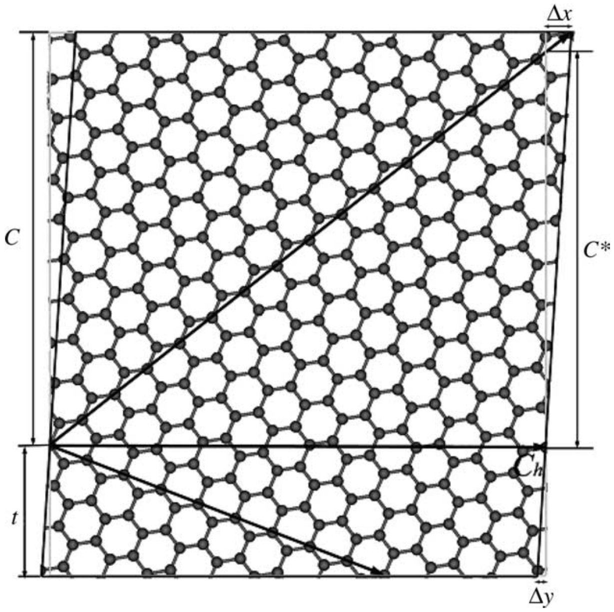

Fig. 2. Radial projection of a twisted carbon nanotube. The light-lined rectangle and the dark-lined parallelpiped are the graphene cut before and after twisting. The twisting angle is reflected as the displacement of atoms such as Δx and Δy in graphene. C_h denotes the magnitude of the perimeter vector of the nanotube which is independent of the twisting angle and $t = ua_0 \sin\alpha$. C and C^* are the pitch lengths of the constituting carbon helices before and after twisting the carbon nanotube, respectively.

$$l = (u+2v)(K_1+K_2)n + 2K_2(u^2+v^2+uv)m, \tag{4}$$

where the periodicity of the twisted carbon nanotube has been expressed by $c^* = uMK_2c$, which is not necessarily the primary periodicity of the nanotube in the axial direction.

The scattering amplitude for the twisted carbon nanotube can be calculated by considering the geometric relationships between the twisted helices in the nanotube as shown in Fig. 2. Although the constituting hexagons are deformed due to the twisting, the total surface area of the nanotube remains unchanged if there is no buckling ever occurred during the twisting process. Therefore, a carbon nanotube (u, v) still consists of u pairs of properly arranged helices as the untwisted nanotube. Choosing one pair of helices as a reference, the rotational and translational shifts of all the helix pairs can be expressed (cf. Fig. 2) as

$$\begin{cases} \varphi_j = \dfrac{2\pi j}{C_h}\left(a_0\cos\alpha - \dfrac{a_0\sin\alpha}{\tan(60^\circ-\alpha)}\dfrac{\Delta\vartheta}{2\pi}\right), \\ z_j = -ja_0\sin\alpha, \end{cases} \tag{5}$$

where the subscript j ranges from 0 to $u-1$ covering all the u pairs of helices constituting the nanotube. By inserting Eq. (5) into Eq. (1) and expressing the helical angle α by the chiral indices (u, v), we can obtain the scattering amplitude for a twisted carbon nanotube as

$$F_{uv}(R,\Phi,l) = \sum_{n,m} f\chi^*_{uv}(n,m)\gamma_{uv}(n,m) \times \exp\left[\mathrm{i}n\left(\Phi+\frac{\pi}{2}\right)\right]J_n(\pi dR), \tag{6}$$

where $\chi^*_{uv}(n,m)$ is a function depending on the nanotube helicity and the detailed bonding between neighboring carbon atoms in the twisted hexagons, and

$$\gamma_{uv}(n,m) = \frac{1-\exp[-2\pi\mathrm{i}(n+mv_j)]}{1-\exp\left[-2\pi\mathrm{i}\left(n+mv_j\right)/u_j\right]} = \begin{cases} u_j, & \text{if } (n+mv_j)/u_j = \text{integer}, \\ 0, & \text{otherwise.} \end{cases} \tag{7}$$

Eq. (6) is very similar to the scattering amplitude of untwisted carbon nanotubes with the exception of $\chi^*_{uv}(n,m)$, which only plays a minor role in determining the electron diffraction patterns of a carbon nanotube.

3. Results and discussion

Fig. 3a shows a high-resolution transmission electron microscopy image of an untwisted carbon nanotube. The diameter of this nanotube is measured to be 1.81 nm from the two dark fringes corresponding to

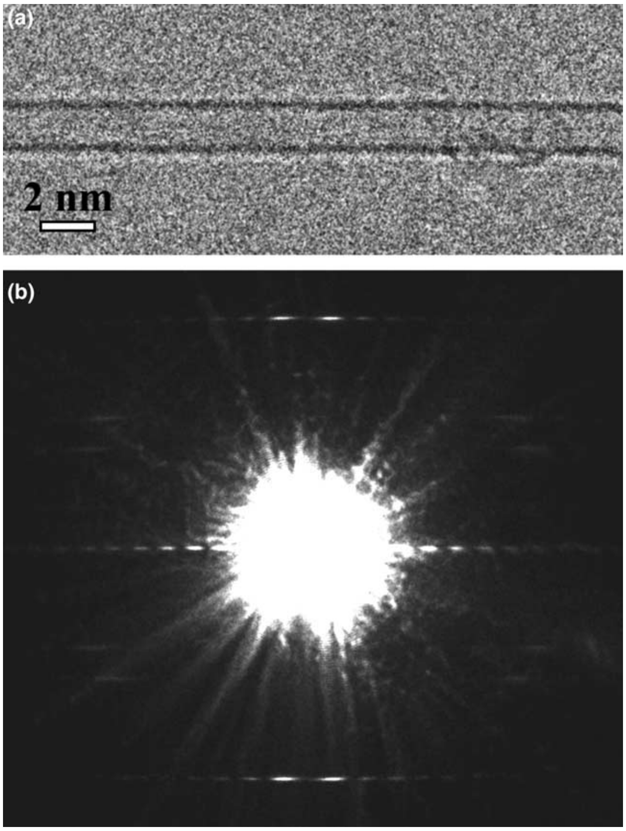

Fig. 3. (a) High-resolution transmission electron microscopy (HRTEM) image and (b) electron diffraction pattern of a single-walled carbon nanotube of chiral indices (*22*,*2*) without twisting.

the projection of side walls in the image. The electron diffraction pattern of this nanotube is shown in Fig. 3b, with the three principal layer lines l_1, l_2, and l_3 indicated in Fig. 4a. The chiral indices of this nanotube are determined to be (*22*,*2*) and this nanotube is a semiconducting nanotube.

Twisting the carbon nanotube of chiral indices (u, v) about its tubule axis changes the atomic positions of carbon atoms, although Eq. (7) dictates that the diffraction intensity distribution on the principal layer lines l_1, l_2 and l_3 for the twisted nanotube are modulated by the same Bessel functions as those for the untwisted nanotube [14]. However, the axial periodicity in the electron diffraction pattern of a twisted carbon nanotube (Eq. (7)) is different from that of the corresponding untwisted carbon nanotube. As a result, the ratio of layer line spacings between the principal layer lines changes. The twisting angle $\Delta\vartheta$ can be expressed in terms of the chiral indices (u, v) and the layer line spacings D_1 and D_2 as shown in Fig. 4a

$$\frac{\Delta\vartheta}{2\pi} = \frac{\varsigma_0 - \varsigma}{\varsigma + v/u}, \tag{8}$$

where we have defined $\zeta_0 = (2u + v)/(u + 2v)$ and $\varsigma = D_1/D_2$ with D_1 and D_2 being measured from the electron diffraction pattern of the twisted nanotube. Since the layer line spacings can be measured very accurately, high accuracy measurement of the twisting angle of a twisted carbon nanotube can be achieved by using electron diffraction technique.

To demonstrate the results discussed above, electron diffraction patterns of a twisted carbon nanotube (*22*,*2*) with right handedness has been performed. Fig. 4a shows the simulated electron diffraction pattern from the untwisted carbon nanotube (*22*,*2*), which is plotted

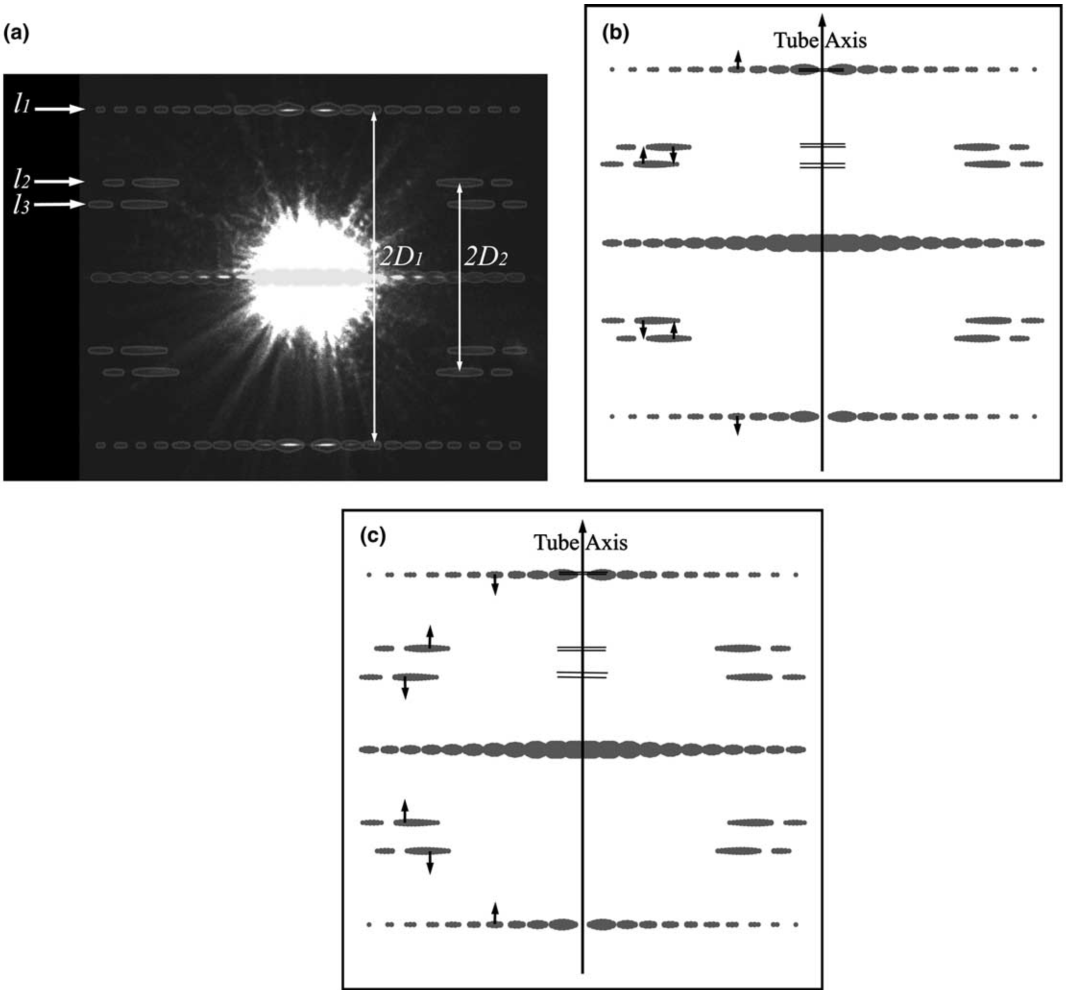

Fig. 4. (a) Simulated electron diffraction pattern of carbon nanotube (*22*,*2*) plotted on the experimental diffraction pattern shown in Fig. 3b. No twisting was applied to the nanotube. (b) Simulated electron diffraction pattern of carbon nanotube (*22*,*2*) twisted counterclockwise ($\Delta\vartheta = -1.20°$/nm). (c) Twisted clockwise ($\Delta\vartheta = +1.20°$/nm). The dark lines on the central line mark the positions of the principal layer line of the nanotube with and without twisting, respectively.

on the experimental electron diffraction pattern. Since carbon nanotube (*22*,*2*) is a chiral nanotube, twisting it about the tubule axis clockwise is different from twisting it counterclockwise as seeing top-down against the tubule axis as schematically illustrated in Fig. 1a. Fig. 4b,c are the simulated electron diffraction patterns of the nanotube twisted counterclockwise (left) and clockwise (right), respectively. It is noticeable that in comparison with the layer lines from untwisted carbon nanotube, indicated by the horizontal lines in the respective figures, the ratio of the layer line spacings D_1/D_2 in Fig. 4b increases due to the repulsive shifting of the layer lines l_1 and l_2, whereas D_1/D_2 in Fig. 4c decreases because of the attractive shifting of the layer lines l_1 and l_2. However, we can observe that the peak positions in the diffraction intensities on all the layer lines remain the same. This allows us to derive u and v by measuring the ratio of the peak positions in the intensity distributions on layer line l_1 and l_2, respectively. With reference to Eq. (8), we can then derive the twisting angles of the twisted nanotube shown in Fig. 4b are −1.20°/nm and +1.20°/nm for the twisted nanotube shown in Fig. 4c. The positive sign denotes clockwise twisting.

For an enantiomorphic pair of nanotubes, i.e., (*22*,*2*) and (*2*,*22*), the diffraction layer lines would shift in opposite directions when they are twisted in the same direction. Therefore, by twisting a chiral nanotube, we are able to detect the handedness of the carbon nanotube. For example, we can assign the nanotube (*22*,*2*) presented above as right-handed, because the layer lines l_1 and l_2 in Fig. 4b shift away from each other when we twist the nanotube counterclockwise. However, under the same counterclockwise twisting, if the layer lines l_1 and l_2 shift towards each other as shown in Fig. 4c, we can tell that the nanotube as left-handed.

In practical applications of this method, the twisting angles are not necessarily as large as shown in the previous example (1.20°/nm), in which a large twisting was chosen for the sake of computational convenience. Measuring the twisting angle by using Eq. (8) is very accurate and the uncertainty can be less than 0.1°/nm due to the high accuracy in the measurement of the chiral indices (u,v) and the layer line spacings in the electron diffraction pattern.

In comparison with other methods, the electron diffraction technique presented here has the advantage of measuring the atomic structures of both untwisted and twisted carbon nanotubes all at one time and it is very rapid and reliable. The method discussed in this Letter can also be extended to determining the handedness of each shell of multiwalled carbon nanotubes.

Some progress has been made in manipulating carbon nanotubes and engineering them as a key component of the nanoelectromechanical system (NEMS) [17–19]. These techniques could be used to twist carbon nanotubes. Although there has been report on the observation and characterization of twisted carbon nanotubes by using scanning tunneling microscopy (STM) technique [20], measuring the twisting angle with this method is far from straightforward and reliable.

4. Conclusions

A practical approach has been established to measure the handedness of chiral carbon nanotubes by using electron diffraction. Twisting a chiral carbon nanotube results in a change of the layer line spacings in the electron diffraction pattern, although the diffraction intensity distribution on the layer lines remains the same. The handedness of a chiral carbon nanotube can be assigned by observing the direction of the shifts of the layer lines before and after twisting of the nanotube. All structural parameters (diameter, helicity, and handedness) of a carbon nanotube can therefore be now determined from one electron diffraction pattern.

References

[1] S.J. Tans, A.R.M. Verschueren, C. Dekker, Nature (London) 393 (1998) 49.
[2] M. Bockrath, D.H. Cobden, P.L. McEuen, N.G. Chopra, A. Zettl, A. Thess, R.E. Smalley, Science 275 (1997) 1922.
[3] P.G. Collins, A. Zettl, H. Bando, A. Thess, R.E. Smalley, Science 278 (1997) 100.
[4] N. Hamada, S. Sawada, A. Oshiyama, Phys. Rev. Lett. 68 (1992) 1579.
[5] R. Saito, M. Fujita, G. Dresselhaus, M.S. Dresselhaus, Phys. Rev. B 46 (1992) 1804.
[6] J.W. Mintmire, B.I. Dunlap, C.T. White, Phys. Rev. Lett. 68 (1992) 631.
[7] A. Rochefort, P. Avouris, F. Lesage, D.R. Salahub, Phys. Rev. B 60 (1999) 13824.
[8] L.-C. Qin, T. Ichihashi, S. Iijima, Ultramicroscopy 67 (1997) 181.
[9] J.M. Cowley, P. Nikolaev, A. Thess, R.E. Smalley, Chem. Phys. Lett. 265 (1997) 379.
[10] L.-C. Qin, S. Iijima, H. Kataura, Y. Maniwa, S. Suzuku, Y. Achiba, Chem. Phys. Lett. 268 (1997) 101.
[11] J.-F. Colomer, L. Henrard, P. Lambin, G. Van Tendeloo, Euro. Phys. J. B 27 (2002) 111.
[12] M. Kociak, K. Suenaga, K. Hirahara, Y. Saito, T. Nakahira, S. Iijima, Phys. Rev. Lett. 89 (2002) 155501.
[13] M. Gao, J.M. Zuo, R.D. Twesten, I. Petrov, L.A. Nagahara, R. Zhang, Appl. Phys. Lett. 82 (2003) 2703.
[14] Z. Liu, L.-C. Qin, Chem. Phys. Lett. 400 (2004) 430.
[15] L.-C. Qin, J. Mater. Res. 9 (1994) 2450.
[16] A.A. Lucas, V. Bruyninckx, P. Lambin, Europhys. Lett. 35 (1996) 355.
[17] J. Cumings, A. Zettl, Science 289 (2000) 602.
[18] M.F. Yu, B.I. Yakobson, R.S. Ruoff, J. Phys. Chem. B 104 (2000) 8764.
[19] B. Bourlon, D. Christian Glattli, C. Miko, L. Forro, A. Bachtold, Nano Lett. 4 (2004) 709.
[20] W. Clauss, D.J. Bergeron, A.T. Johnson, Phys. Rev. B 58 (1998) 4266.